Title
p38 MAP Kinase Regulates Remodeling of Heart via IRE1α During Early Postnatal Development

Author
Li, Jin

Publication Date
2016

Peer reviewed|Thesis/dissertation

UNIVERSITY OF CALIFORNIA
Los Angeles

p38 MAP Kinase Regulates Remodeling of Heart via IRE1α During Early Postnatal Development

A thesis submitted in partial satisfaction of the requirements for the degree Master of Science in Physiological Science

by

Jin Li

2016

ABSTRACT OF THE THESIS

p38 MAP Kinase Regulates Remodeling of Heart via IRE1α During Early Postnatal Development

by

Jin Li

Master of Science in Physiological Science

University of California, Los Angeles, 2016

Professor Yibin Wang, Co-Chair

Professor Xinshu Xiao, Co-Chair

Previous studies show mammalian cardiomyocytes will undergo depressed proliferation and induced apoptosis shortly after birth, but vary to different degrees in two ventricles. p38 MAP kinase (p38) was indicated to be a contributor to this variation, but with unclear functioning mechanism. For a better understanding, we conducted *in vivo* study using p38α/β cardiac specific conditional knockout mice model, and *in vitro* experiments in neonatal rat ventricular cardomyocytes. Both models show inhibiting p38α/β causes an increased expression of inositol-requiring protein 1 alpha (IRE1α) and x-box binding protein 1 (XBP1) splicing in cardiomyocytes, but different pro-survival responses at different postnatal days: elevated mitosis at P3 while reduced apoptosis at P1, while both responses were found in vitro. Overexpressing IRE1α *in vitro* generates similar pro-survival effect to p38 inhibition, whereas knocking down

XBP1 significantly blunts p38-inhibition-induced proliferation. Thus, we raise a chamber-specific model in which p38 regulates postnatal heart proliferation/apoptosis via inhibiting IRE1α.

The thesis of Jin Li is approved.

James G Tidball

Yibin Wang, Committee Co-Chair

Xinshu Xiao, Committee Co-Chair

University of California, Los Angeles

2016

Table of Contents

Acknowledgements

Although only my name is mentioned on the cover of this thesis, a variety of people have contributed to make it possible. I would like to give my great gratitude to all of them, without whom my thesis study and graduate experience would have never been so meaningful and cherishable.

My deepest appreciation is to my thesis mentor Dr. Yibin Wang. He is not only a great scientist of insight, guiding me towards rigorous and profound investigations, but also a life-long teacher who always offers generous instructions to help me achieve my goal. I am very fortunate to be one of Dr. Wang's students.

My committee members Dr. Xinshu Xiao and Dr. James G Tidball, have been always been there to listen and give me advice. I am deeply grateful to their kind support and careful reading. I am also very thankful to their spending time and efforts making revisions of the thesis abstract for me.

My supervisor Dr. Tomohiro Yokota has always been there to offer me practical advice and help me with careful revisions. I am very grateful to Dr. Yokota for generously sharing his work with

me for my thesis writing. Besides, Dr. Yokota is a great master teaching me a good many of bio-techniques and beers.

I am also grateful to my lab colleague Dr. Chen Gao, for her always kind-hearted help to both my thesis study and graduate life. I felt fortunate to have worked and made good friends with her.

I am also very thankful to all my other lab colleagues as following, for their kind support both from and outside work during my graduate study. Dr. Zhihua Wang, Dr. Christoph Rau, Dr. Marlin Touma, Haiying Pu, Jing Gao, Shuxun Ren, Haipeng Sun, Xuedong Kang, Yan Zhao, Jim OHearn, Josh Lee, He Wang, Mengping Chen, Rozeta Avetisyan, Ye Zhang and Yang Song.

Most importantly, none of this would be possible without the love and great support of my family. Studying abroad is not so easy, and thanks to their concerns and encouragement, I have made great improvement and very enjoy this experience.

1. INTRODUCTION

Shortly after birth, mammalian cardiomyocytes undergo depressed proliferation activity compared to in the fetal period (Engel et al., 2005). Strikingly, this cardiac remodeling is chamber-specific in neonatal mice, with the cardiomyocytes in the right ventricle (RV) even less proliferative but more apoptotic compared to those in the left ventricle (LV), leading to distinct size and cell numbers of two ventricles (Fernandez, Siddiquee, & Shohet, 2001; Yokota, Ren, & Wang, 2014). However, so far most studies have only focused on the LV, to interpret the molecular mechanism underlying this chamber-specific remodeling, but had barely little understanding on the RV.

p38 mitogen-activated protein (MAP) kinase (p38) is a prominent regulator to inhibit mitosis and stimulate differentiation, apoptosis and inflammation in numerous cell types (Nebreda & Porras, 2000; Rose, Force, & Wang, 2010). It is also shown that p38 is a predominant suppressor in mice cardiomyocytes proliferation (Engel et al., 2005). p38 MAP kinase has four identified isoforms, in which p38α and p38β are the main isoforms existing in heart (Groenendyk, Sreenivasaiah, Kim, Agellon, & Michalak, 2010). The mitosis of neonatal cardiomyocytes in mice can be greatly induced by p38α cardiac-specific conditional knockout (cdKO)(Engel et al., 2005). Furthermore, a RV-specific proliferation induction is seen when knocking out both p38α andβ in neonatal heart (Yokota et al., 2014).

On the other hand, p38 inhibition is reported to reduce cardiomyocytes apoptosis under numerous modes of stress (Ma et al., 1999; Sun et al., 2006). Therefore, it is very worthwhile to study the downstream pathway of p38 MAP kinase, in mediating cardiomyocytes remodeling in postnatal heart. Here, we propose a potential mechanism of p38 MAP kinase induces neonatal cardiomyocytes proliferation whereas represses their apoptosis through the induction of inositol-requiring protein 1 alpha (IRE1α).

IRE1α serves as an endoplasmic reticulum (ER) transmembrane protein kinase and an endoribonucleases (RNase), which can respond to ER stresses by altering gene expression, via unfolded protein response (UPR) (Groenendyk et al., 2010; Hetz & Glimcher, 2009; Thuerauf et al., 2006; X. S. Wang et al., 1997). Interestingly, IRE1α acts as a cell fate executor via both pro- and anti-apoptosis pathway. Studies show that this cell fate switch model is achieved by two enzymatic activities of IRE1α, its RNase activity on splicing x-box binding protein 1 (XBP1) and kinase activity on autophosphorylation once activated (Chen & Brandizzi, 2013; Han et al., 2009). On the one hand, once sensing ER stresses, IRE1α launches its RNase activity on the mRNA of XBP1, by excising a 26-nucleotide intron from the latter to generate a spliced isoform (sXBP1) (Groenendyk et al., 2010; Han et al., 2009). sXBP1 is a transcription factor which is known to promote prosurvival gene expressions in many cell types, such as enhancing the proliferation of cancer cells and pancreatic β cells (Romero-Ramirez et al., 2004; Thorpe & Schwarze, 2010; Xu et al., 2014), and represses

apoptosis in cardiomyocytes under stress (Z. V Wang et al., 2014). On the other hand, however, IRE1α's kinase activity is more proapoptotic. Thus, this complex while fine-tuned cell fate control by IRE1α is essential for us to understand any IRE1α-associated cell remodeling mechanism. In our model, we demonstrated the general effect of p38-inhibition-induced IRE1α activity is mostly the RNase activity, making a pro-survival contribution to neonatal cardiomyocytes.

2. METHODS

Transgenic mice model

The construction of the cardiac-specific p38 α and β isoforms conditional knockout mice was referred to our lab's collaborated paper (Liao et al., 2001), except that the floxed crossing line is changed into p38α and β floxed alleles in our model.

Cell culture

Neonatal rat ventricular myocytes (NRVMs) isolated from postnatal day 0 to day 3 were prepared as previously described (Streicher, Ren, Herschman, & Wang, 2010), and maintained in DMEM supplemented with 1% Insulin-Transferrin-Selenium (ITS-G) (BD Biosciences), 100 U/mL penicillin and 100 μg/ml streptomycin for 24h before infection or drug treatment. P38 inhibition cells were then treated with SB202190 (10μM) (Cell

Signaling) and IRE1α overexpression cells were infected with adenovirus at a multiplicity of infection of 100 particles per cell 2 days before harvesting.

RNA and Protein extraction

Dissected hearts were separated in four chambers and free-wall of the RV and LV were used for RNA or protein extraction. Total RNA was extracted from tissue or cultured NRVMs using TRIzol reagent (Life technologies) in accordance with the manufacturer's instructions. Nuclear and cytoplasmic RNA were extracted using Cytoplasmic & Nuclear RNA Purification Kit (Norgen Biotek) in accordance with the manufacturer's instructions. Total protein was extracted as mentioned previously (Zhou, Lu, Gao, Wang, & Sun, 2012).

Quantitative real-time PCR (qPCR) analysis

Procedures were conducted as our lab's previous methods (Monte et al., 2013)

Primers used in this study are as follows: The forward primer specific for mosue/rat IRE1α was 5'-tctggggaagtggggcgcat-3'. The reverse primer specific for mosue/rat IRE1α was 5'-agcaaaggaagagtgctgcctcg-3'. The forward primer specific for rat s/uXBP1 was 5'-ctcagaggcagagtccaagg-3'. The reverse primer specific for rat s/uXBP1 was 5'-acagggtccaacttgtccag-3'. The forward primer specific for rat ki67 was 5'-atcattgaccgctcctttaggt-3'. The reverse primer specific for rat ki67 was 5'-gctcgccttgatggttcct-3'. The forward primer specific for rat Aurora B was

5’-aaatccaggcgcacctgaaacatc-3’. The reverse primer specific for rat Aurora B was 5’-agcaggttctccggctttatgtct-3’. The forward primer specific for mouse 18s was 5’-aggccctgtaattggaatgagtc-3’. The reverse primer specific for mouse 18s was 5’-gctcccaagatccaactacgag-3’. The forward primer specific for mouse 18s was 5’-aggccctgtaattggaatgagtc-3’. The reverse primer specific for mouse 18s was 5’-gctcccaagatccaactacgag-3’. The forward primer specific for rat Gapdh was 5’-atgggaagctggtcatcaac-3’. The reverse primer specific for rat Gapdh was 5’-ccacagtcttctgagtggca-3’.

Immunofluorescence staining

NRVMs were plated on gelatin-coated cover glass. Treated cells were fixed by 4% paraformaldehyde/PBS. Fixed cells were hybridized with anti-ki67 (abcam, 1:200) and anti-Tropomyosin (Sigma Aldrich, 1:200) for overnight at 4C. Cells were then hybridized with fluorescence-conjugated secondary antibody for 2 hrs. Nuclei were counterstained with Hoechst 33342 (Life Technologies, 1:1000) for 30 mins. Images were taken with confocal microscope (Nikon) and analyzed from at least 200 NRVMs.

Terminal deoxynucleotidyl transferase dUTP Nick-End Labeling (TUNEL) assay

TUNEL assay was conducted using the In Situ Cell Death Detection Kit, POD (Roche). Cells were incubated for 15 mins after hybridized with fluorescence-conjugated secondary antibody for 2 hours. Cells treated with DNase (Qiagen) served as positive controls.

Western blot

Western blot were procedured following our lab's previous paper (Zhou, Lu & Gao et al. 2012). The blot was probed by the following primary antibodies, p38 MAP kinase (Cell Signaling, 1:1000), phospho-p38 (Thr180/Tyr182) (Cell Signaling, 1:1000) and cleaved Caspase 3 (Asp175) (Cell Signaling, 1:500); IRE1α (Santa Cruz, 1:250), Bcl2 (C-2) (Santa Cruz, 1:500) and actin (Santa Cruz, 1:250).

Statistical analysis

Group comparisons are done using Student's t-test. A p-value less than 0.05 was defined as significantly.

3. RESULTS

p38αβ cdKO induces cardiomyocytes proliferation and XBP1 splicing at P3 in the RV

The MAP kinase will exert maximum enzymatic activity only in their phosphorylation state (Johnson, Noble, & Owen, 1996), therefore, the phosphorylation ratio of MAP kinase can serve as a good indicator of their enzymatic activities Firstly, we examined the phosphorylation ratio of p38 MAP kinase in two neonatal ventricles in order to visualize its maximum activity. These western blot data were credited to my collaborator Tomohiro Yokota (Figure 1 A, B and C). Yokota's data suggest a similar p38 activation level in the two ventricles at postnatal day 1, while as the neonatal mice developed from P3 through P7, this level favors to the RV to more than 4 fold. This distinctive p38 activation is consistent with the chamber-specific proliferation activity: both ventricles undergo mitosis suppression from P3, but the repression in the RV is more sever than that in the LV (Yokota et al., 2014). Furthermore, RNA-seq were performed in the wild type (WT) and p38αβ cdKO two ventricles at P3, and the results suggest a large variety of genes participated in the mitotic pathway undergo up-regulating expression in the RV of p38αβ cdKO mice (Figure 2A), in support of Yokota's western blot results. Therefore, we confirm that shortly after birth, p38 MAP kinase serves as a predominant regulator of cardiomyocytes' proliferation activity, in a chamber-dependent manner.

We then use the Whole Genome-Rvista software to analyze our RNA-seq data, using WT and p38αβ cdKO mice ventricles extracted from P1 and P3. Four candidate gene lists were generated from this analysis, sorted by their potentials to serve as a downstream target of

p38. Interestingly, a UPR-associated gene XBP1 was found to be highly ranked in both ventricles at P1, but only in the RV at P3 (Figure 2B). As we stated in the introduction, spliced XBP1 is known as a transcription factor promoting the expressions of many pro-survival genes. Thus, we assume that XBP1, or spliced XBP1 specifically, is very likely to work as a downstream target of p38, responsible for the p38αβ-cdKO-induced proliferation in the RV at P3. Hence, we further confirmed our hypothesis by conducting a qPCR in both ventricles generated from P3, to check their nuclear XBP1 splicing level respectively. We identified that the sXBP1 amount in the RV is significantly lower than that in the LV. As expected, this splicing reduction in the RV is specifically attenuated by p38αβ cdKO (Figure 2C), which provides strong evidence of sXBP1's involvement in this p38-regulated pathway.

p38 inhibition promotes proliferation and XBP1 splicing in NRVMs

To support our *in vivo* findings, we treated NRVMs *in vitro* with SB202190, an inhibitor to p38α and β. Mitosis activities are measured by ki67 expression levels using immunostaining (Figure 3A). Analysis results show that p38 inhibition can promote neonatal cardiomyocytes proliferation. XBP1 splicing level was also measured by qPCR, also revealing a significant increase after p38 inhibition treatment (Figure 3B and 3C). Therefore, we consider that sXBP1serves as downstream target of p38 MAP kinase, involved in the neonatal cardiomyocyte cell cycle regulation.

p38αβ cdKO increases IRE1α expression at P3 in the RV

The splicing level of XBP1 mRNA can be mediated by two ER sensors in the UPR: activating transcription factor 6 (ATF6) can induce total XBP1, while IRE1α can enhance only XBP1 splicing by exerting its RNase activity(Yoshida, Matsui, Yamamoto, Okada, & Mori, 2001). We then would like to investigate whether any of these ER sensors is correlated with the increment of XBP1 splicing level in the RV, resulted from p38αβ cdKO. Thus, we analyzed the expression level of ATF6 and IRE1α in neonatal cardiomyocytes respectively. qPCR data suggest that when the cdKO mice entered P3, IRE1α mRNA expression undergoes a significant reduction only in their RV but not the LV compared to respective ventricle of the WT mice (Figure 4B). In contrast, for these cdKO mice at P3, our RNAseq data indicate that ATF6 expression only varies in the LV but not the RV, which is inconsistent with our observed RV-specific proliferation and XBP1 change at this postnatal day after knocking out p38. Therefore, we initially conclude that it is IRE1α rather than ATF6 that is responsible for this induced XBP1 splicing caused by p38αβ cdKO.

p38 inhibition enhances IRE1α expression in NRVMs

The IRE1α expression level was also measured *in vitro*. qPCR data suggests that p38 inhibition induces a significant increase in IRE1α expression (Figure 3D). And this induction can further accumulate to the effect resulted from IRE1 overexpression which was conducted by adenovirus infection. Hence, we conclude that the increased XBP1 splicing resulted from p38 inhibition is mediated through an enhancement in IRE1α expression.

Therefore, in order to further prove our finding, we then would like to study the molecular response to IRE1α overexpression in NRVM, as a comparison to the response to p38 inhibition.

IRE1α overexpression induces NRVM proliferation

Firstly, we would like to investigate whether IRE1α has a similar effect to p38 inhibition on inducing NRVM proliferation. We conducted two qPCRs in NRVM using both ki67 and Aurora B as proliferation markers, and find out IRE1α overexpression can significantly promote proliferation (Figure 5A). Moreover, we also compared this proliferation enhancement to that caused by p38 inhibition, using immunostaining. Our data indicate the capacity of IRE1α overexpression to greatly elevate cells' proliferation to a similar extend as

p38 inhibition does (Figure 3A). Therefore, these findings add more evidence to IRE1α's possibility to act as mediator.

IRE1α overexpression enhances XBP1 splicing in NRVMs

Secondly, we would like to confirm that the IRE1α-overexpression-induced proliferation is indeed due to spliced XBP1, as a result of the former's increased RNase activity. Using qPCR , we detected a significant rise in the s/uXBP1 ratio in NRVMs due to IRE1α overexpression. This proliferative effect caused by IRE1α overexpression can not only compete with the one caused by p38 inhibition, but can also accumulate to the latter (Figure 3B and 3C).

Furthermore, by using siRNA to knock down XBP1, we were able to more precisely understand XBP1's association with p38. We then transfected NRVMs with siXBP1 or si negative control, and then compared their mitotic activity by both qPCR and immunostaining (Figure 5B and 5C). Our data demonstrate that knocking down XBP1 not only reduces NRVMs' basal proliferation level, but most importantly, it also significantly blunts the mitosis induced by p38 inhibition. Consequently, we conclude that p38 inhibition can promote the proliferation activity of NRVMs by promoting IRE1α's expression, which exerts its RNase up-regulating XBP1 splicing, directly by promoting IRE1α expression.

p38αβ cdKO attenuates apoptosis at P1 in the RV

p38 MAP kinase was also demonstrated to regulate apoptosis (Ma et al., 1999; Y. Wang et al., 1998). Previous study in pig hearts suggests that after birth, the apoptotic activity in two ventricles also varies dynamically all the way through adulthood (Fernandez et al., 2001). Thus, we consider it would be necessary to explore whether the divergent expression of p38 in neonatal mouse hearts is also correlated with a chamber-specific change of apoptosis.

The following *in vivo* apoptosis study was conducted by Tomohiro Yokota (Yokota et al., 2014). Yokota detected the apoptotic activity of neonatal cardiomyocytes in two ventricles in a chronological order, by the Terminal deoxynucleotidyl transferase dUTP Nick-End Labeling (TUNEL) assay. As early as P1, Yokota found a significant divergence of TUNEL positive cells in two ventricles: the percentage of TUNEL positive cells in the RV is more than twice higher than that in the LV (Figure 6A and 6B). However, this divergence vanishes almost to zero as the mice grow to from P1 to P3. Then, Yokota further examined this chamber-specific apoptosis in the conditional knockout mice model, aiming to find out whether this effect was truly due to p38 MAP kinase. It indicates that at P1, p38αβ cdKO could significantly attenuate apoptosis to almost four folds (measured by the percentage of TUNEL-positive cells) in the RV but has no effect in the LV (Figure 6A and 6B). Nevertheless,

as the mice go through P3, p38αβ cdKO does not necessarily cause a change in the low basal apoptotic activity in both ventricles.

Cysteine-aspartic acid protease 3 (Casp3) is an important member in the Caspase family, which plays a central role in the execution-phase of cell apoptosis (Fan, Han, Cong, & Liang, 2005). Once activated, the cleaved form of Casp3 (cCasp3) serves as an effector in the programmed cell death cascade, thus the abundance of cCasp3 is widely used as an indicator of cell apoptotic activity (BD biosciences. 2012). The B-cell lymphoma 2 (Bcl2) family expresses a set of proteins which can regulate cell death, exerting either an anti- or pro-apoptotic effect. Bcl2 works as an anti-apoptotic gene in this family, and even slight variance in its gene expression level can lead to a change in programmed cell death level (Tsujimoto, 1998). Therefore, the expression levels of cCasp3 and Bcl2 are good indicators of cell apoptotic activity.

Yokota further checked the protein abundance of cCasp 3 and Bcl2 (relative to actin respectively) in both WT and p38αβ cdKO mice hearts at P1. His western blot data show that in WT ventricles, the cCasp3 expression level in the RV is higher than that in the LV (Figure 6D). In addition, knocking out p38αβ sequesters the expression of cCasp3 to more than two folds in both chambers, with that in the RV more significant. In terms of the Bcl2 protein expression, it has a just opposite trend as cCasp3, in which the Bcl2 abundance is

over twice less in the RV than the LV in the WT mice (Figure 6E). Whereas after knocking out p38αβ, Bcl2 experiences an obvious expression rise in the RV, but this increase was not observed in the LV. Overall, these western blot data imply a chamber-specific apoptosis in mice hearts at P1. Additionally, p38 MAP kinase plays unequal roles in two ventricles' apoptotic levels: p38 is a pro-apoptotic kinase in the neonatal ventricles, but has a stronger effect in the RV compared to the LV.

Besides, RNA-seq data provide further evidence by listing genes undergo down-regulation at P1 resulted from p38αβ cdKO. The list suggests that a set of genes in the RV exerting positive regulation of apoptosis were undergoing significant expression attenuation (Figure 6C), but this gene set was not observed in the RNA-seq data from the LV. Thus, we further confirm our finding and lead to a conclusion that p38αβ cdKO can reduce the ventricle apoptosis at P1, but only in the RV.

p38 inhibition reduces hydrogen-peroxide-induced NRVM apoptosis via enhancing IRE1α expression

Similarly, we investigated the pro-apoptotic role of p38 MAP kinase using NRVMs *in vitro*. TUNEL assay suggests that p38 inhibition can reduce the basal apoptotic activity to almost a half extend compared to the non-treated (NT) NRVMs (Figure 7), which is consistent with

Yokota's *in vivo* data. But considering this basal apoptotic activity is not very high, we thought it might be more interesting and necessary to further study how these cells respond to p38 inhibition upon stress.

Our data suggest that IRE1α undergoes a p38-depedent expression in neonatal cardiomyocytes, and because IRE1α is an ancient and well-studied endoplasmic reticulum (ER) stress sensor, we presume that the mechanism underlying p38αβ-cdKO-suppressed apoptosis in neonatal cardiomyocytes may be based on the unfolded protein response (UPR) triggered by ER stress. Therefore, we would like to narrow down our choice to only ER stress stimulators to simulate this stress condition. Hydrogen peroxide (H2O2) is a widely-used oxidant to evoke ER stress thus causing cell death in many cell types (Buttke & Sandstrom, 1994; Pierre et al., 2014). Previous study also shows that the exact cell death mechanism caused by H2O2 treatment is dose-dependent: low dose (10 to 100 uM) H2O2 is a good mediator to stimulate apoptosis, while higher dose of H2O2 will instead evoke necrosis (Lennon, Martin, & Cotter, 1991). Hence, to better understand how p38 affect NRVMs' apoptosis in a stressful environment, we would like to induce cell apoptosis, by applying just 100 uM H2O2 to NRVMs and treated them for 0.5 hour before harvesting,

Our data show that half-hour H2O2 treatment is able to generate an extremely high-level of apoptosis up to 98.3% (Figure 7). Strikingly, this death rate can be greatly reduced to as

much as 23.6% once cells are applied with p38 inhibitor (applied one hour before H2O2 treatment). This effective rescue effect indicates that the pro-apoptotic effect of p38 MAP kinase on neonatal cardiomyocytes is not only existed in the basal condition, but is even more critical upon acute stress.

As we mentioned above, IRE1α possesses a high potential of acting as a downstream regulator in this p38-dependent apoptosis pathway as well. The cell fate control model of IRE1α can switch between pro- and anti-apoptosis. Interestingly, upon ER stress, the RNase activity is responsible for XBP1 splicing only, contributing to cell survival; whereas its kinase activity is responsible for mRNA decay that will usually override XBP1 splicing, leading to apoptosis (Chen & Brandizzi, 2013; Han et al., 2009).

Therefore, we next would like to study whether and how IRE1α can regulate apoptosis in NRVM under both basal and stress circumstances. We overexpressed IRE1α in NRVMs as a comparison to the LacZ overexpression and p38 inhibition groups respectively. Our TUNEL assay data show that IRE1α overexpression can not just suppress programmed cell death to almost 0% in the normal condition, but upon H2O2 stress simulation, it serves as a vital rescuer to reduce cardiomyocytes apoptosis even down to the non-stressful basal level (5.7%) (Figure 7). Therefore, we are able to conclude that p38 MAP kinase inhibition can attenuate apoptosis of neonatal cardiomyocytes, through enhancing IRE1α expression. And

since the effect caused by IRE1α overexpression is pro-survival, we hypothesized that this enzymatic activity is most likely to be RNase instead of kinase. But more experiments are required to be done to further support our hypothesis.

4. DISCUSSION

Based on our findings, we propose a model on how p38 MAP kinase regulates neonatal hearts remodeling via IRE1α (Figure 8). The proliferation and apoptosis pathways in this model share similar regulators of IRE1α and sXBP1, but diverge into two branches to exert different modes of pro-survival effect. More detailedly, after knocking out p38α/β isoforms in the mice right ventricle (RV), or once inhibiting p38 expression in the NRVMs, there is a universal induction in IRE1α expression and consequently an increasing XBP1 splicing level. However, this enhanced XBP1 splicing will turn on different mechanisms to promote neonatal cardiomyocytes survival in the RV at different time point: increased sXBP1 leads to an increment of proliferation only at P3, while results in reduced apoptosis only at P1. But both of these increased mitosis and suppressed apoptosis regulations exist in the NRVMs. In other words, the dynamic and RV-specific elevated apoptosis at P1 and reduced proliferation at P3 share a similar remodeling mechanism, both due to p38 MAP kinase sequestering IRE1α expression, and the consequent attenuation of IRE1α's RNase activity

on splicing XBP1. But in terms of NRVMs, since they are a mixture of cardiomyocytes isolated from both ventricles from P0 to P3 (Streicher et al., 2010), it is reasonable to expect these time and chamber-specific anti-survival regulation pathways both exist in NRVMs.

IRE1α is one of the three noted ER stress sensors in cells, which is able to promote cell survival by reducing misfolded protein levels. In order to achieve that, IRE1α launches its RNase activity on the RNA of XBP1, by excising a 26-nucleotide intron from the latter to generate a spliced isoform (sXBP1) (Groenendyk et al., 2010; Han et al., 2009). As a transcription factor, sXBP1 is known to promote a good many of pro-survival gene expressions in various cell types, such as enhancing the proliferation of cancer cells and pancreatic β cells (Romero-Ramirez et al., 2004; Thorpe & Schwarze, 2010; Xu et al., 2014), and represses apoptosis in cardiomyocytes under stress (Z. V Wang et al., 2014). Also, a study done by Lin et al demonstrates that IRE1α activities is found out to attenuate during persistent ER stress, but a sustained IRE1α level gained by artificial overexpression can enhance cell survival greatly (Lin et al., 2007). This study also supports our hypothesis of the pro-survival role of IRE1α in neonatal cardiomyocytes. But more development and physiology evidence is required to explain why this pro-survival activity exerts differently in the RV at different postnatal day, by behaves either only anti- or only pro-mitoticly. Moreover, the anti-apoptotic role of sXBP1 in our model in both NRVMs and the RV at P1

has not been strongly confirmed, but is only based on our RNA-seq data (Figure 2D) and the highly-recognized model of IRE1α's governing cell fate (Chen & Brandizzi, 2013; Han et al., 2009). Hence, it is highly suggested a TUNEL assay should be done in the future to check how siXBP1 would affect this p38-inhibition-suppressed apoptosis in NRVMs.

Besides, although both p38 inhibition and IRE1α overexpression can both lead to pro-mitotic and anti-apoptotic effects on NRVMs, it is also undeniable that IRE1α overexpression always performs better than p38 inhibition in these two regulation pathways. Here, on the one hand, we consider that p38 MAP kinase, or p38αβ in precise, may not be the only upstream inhibitor of IRE1α, which may be capable to explain why inhibiting p38αβ alone is unable to evoke all the IRE1α's pro-survival activities. On the other hand, despite the inhibition effect of p38αβ via IRE1α on neonatal cardiomyocytes survival, it is still highly likely for p38αβ to play a positive role in neonatal heart development, in which case suppressing p38αβ totally in NRVMs could meanwhile retard some normal cellular pro-survival mechanisms. Therefore, it is reasonable to observe imperfect concerted pro-survival effects of p38 inhibition and IRE1α overexpression.

Another implication of our study is that the proliferative role of IRE1α in neonatal hearts also promotes our understanding of the regeneration capability of neonatal mammalian hearts. Upon heart injury, adult mammals are unable to regenerate most of the lost

cardiomyocytes like lower vertebrates do (Gamba, Harrison, & Lien, 2014), therefore when the injury is severe, it could lead to heart failures and even death of mammals (Porrello & Olson, 2014), despite recent studies found that partial cardiomyocytes do undergo mitosis during adult life at a decreased annual renovation rate from 1% at age 25 to 0.45% at age 75 in humans. However, unlike adult mammals, neonatal mammals do possess the capability to regenerate cardiomyocytes upon injury (Porrello et al., 2011; Uygur & Lee, 2016). Besides, p38 MAP kinase is demonstrated to be an important regulator of cardiogenesis in zebrafish and mammals (Engel et al., 2005; Jopling, Suñè, Morera, & Belmonte, 2012). One study also suggest the possible involvement of ER-associated pathways in the cardiomyocytes renewal (Groenendyk et al., 2010). Therefore, the pro-survival role of IRE1α in cardiogenesis, which is found by our studies, may provide insights to the downstream pathway of the p38-regulated neonatal cardiac regeneration. Therefore, this study may also be helpful to understand and even alter the incapability of adult cardiogenesis.

5. FIGURES

Figure 1

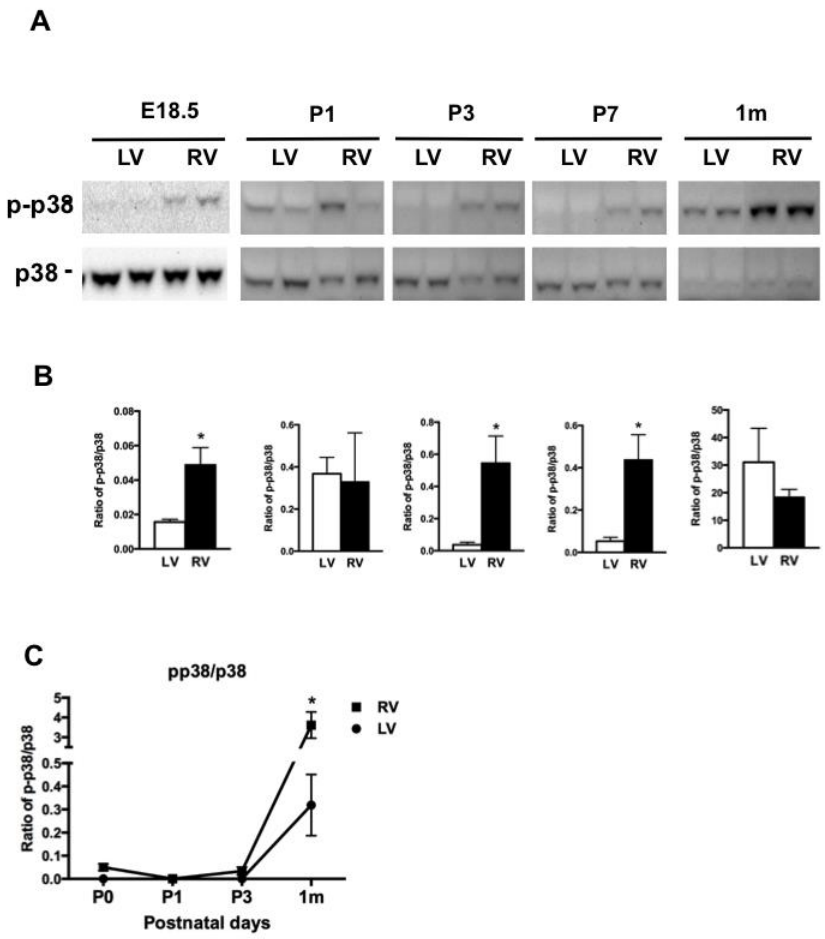

Figure 1. p38 MAP kinase phosphorylation ratio undergoes a chamber-specific and dynamic trend in neonatal hearts (Yokota et al. 2014). (A) Western blot data suggest the p38 MAP kinase phosphorylation ratio is higher in the RV than in the LV only at embryonic day 18.5 (E18.5), postnatal day 3 and day 7, but this ratio does not vary significantly at other time points. (B) and (C) are quantitative results of (A). *p* value (LV vs. RV) * indicates $p<0.05$, n=3.

Figure 2

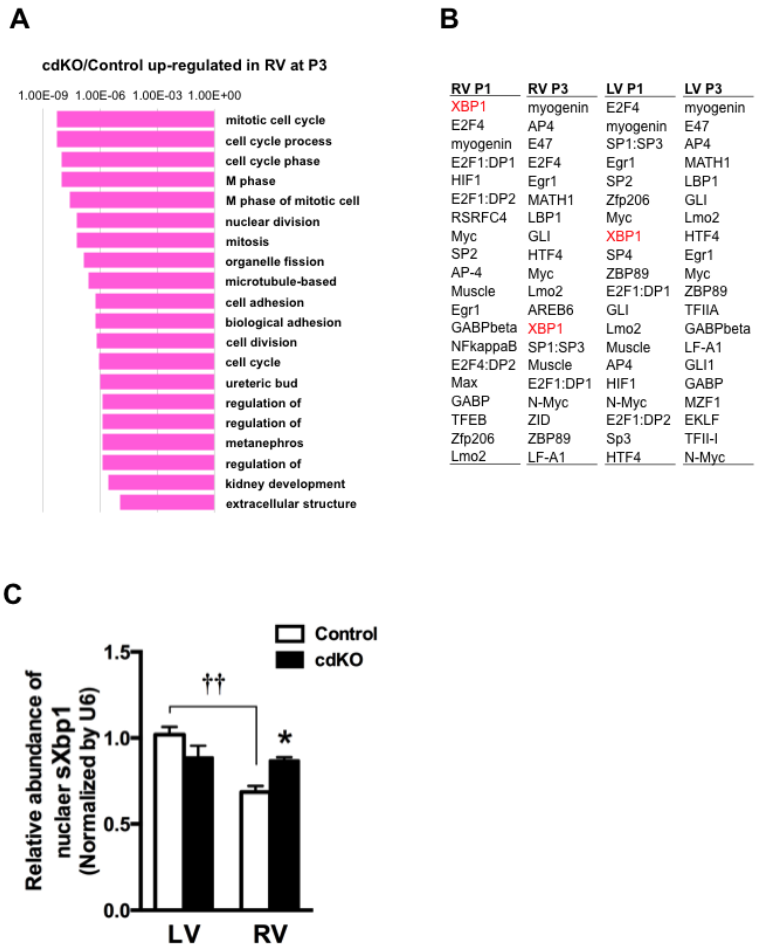

Figure 2. p38αβ cdKO induces cardiomyocytes proliferation and XBP1 splicing at P3 in the RV.

(A) RNA-seq data suggest in the RV of the p38αβ cdKO mice, a set of genes involved in the mitotic pathway undergo up-regulation at P3. Genes in similar pathways were not found to be up-regulated in the LV of the same mice at P3. (B) XBP1 is a predominant candidate downstream regulator in the p38-suppressed proliferation pathway. Whole Genome-Rvista

analysis was applied to our RNA-seq data, comparing both ventricles of the WT and p38αβ cdKO mice extracted from P1 and P3. Candidate gene lists were generated from this analysis, sorted by those genes' potentials to serve as a downstream target of p38. Among them, XBP1 was found to be highly ranked in both ventricles at P1, but only in the RV at P3. (C) qPCR data show p38αβ cdKO causes an induction of nuclear XBP1 splicing level in the RV at P3. In the wild type (WT) mice, the nuclear sXBP1 mRNA abundance is higher in the LV than in the RV, but p38αβ cdKO significantly increases this splicing level only in the RV but not in the LV. *p value* (LV vs. RV) †† indicates $p<0.01$, (control vs. cdKO) * indicates $p<0.05$, n=3.

Figure 3

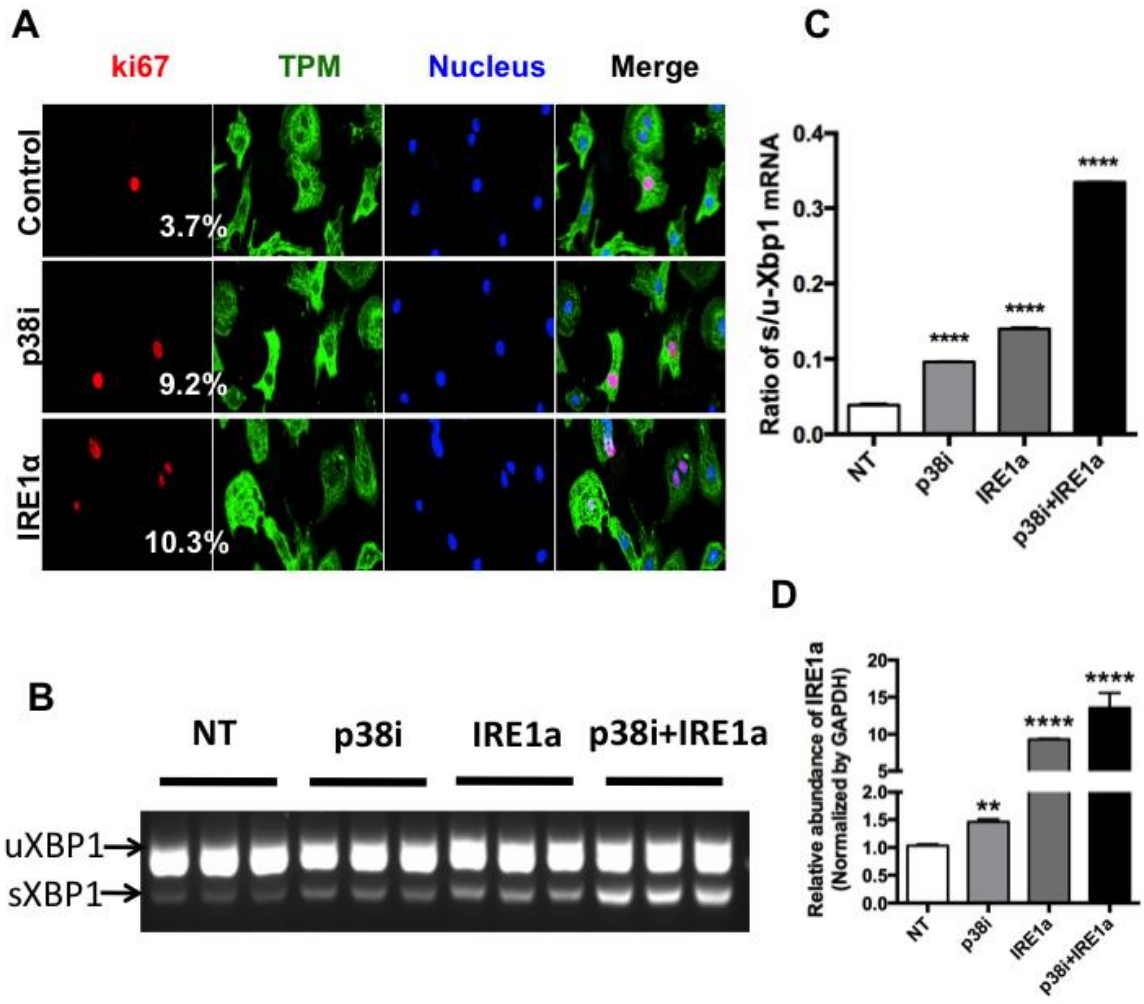

Figure 3. IRE1α overexpression promotes both proliferative activity and XBP1 splicing in NRVMs, to a similar extend as p38 inhibition does. (A) Immunostaining data suggest IRE1α overexpression increases NRVMs' proliferation, similar to p38 inhibition does. Ki67, tropomyocin and 4',6-diamidino-2-phenylindole (DAPI) are used to detect proliferative activity (red), cardiomyocytes (green) and nuclei (blue) respectively. The ratio of ki67 positive cardiomyocytes to total cardiomyocytes is quantified as an indicator of the

proliferation level of cardiomyocytes. (B)(C) qPCR and its quantification data show IRE1α overexpression increases the ratio of s/uXBP1in NRVMs, similar to p38 inhibition does. In addition, this proliferative effect caused by IRE1α overexpression can also accumulate to the one caused by p38 inhibition. (D) qPCR data suggest that p38 inhibition and IRE1α overexpression in NRVMs can both lead to a significant induction of IRE1α mRNA abundance. *p value* (NT vs. p38i, NT vs. IRE1α, NT vs. p38i + IRE1α), ** indicates $p<0.01$, and **** indicates $p<0.0001$, n=3.

Figure 4

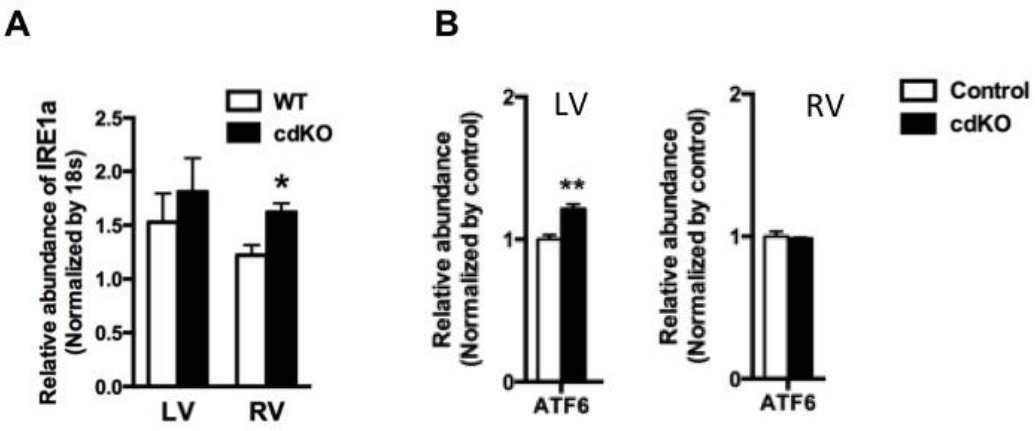

Figure 4. p38αβ cdKO results in a RV-specific IRE1α induction, but LV-specific ATF induction..(A) p38αβ cdKO increases IRE1α mRNA expression only in the RV at P3. qPCR data suggest that when the p38αβ cdKO mice entered P3, IRE1α mRNA expression undergoes a significant reduction only in their RV but not the LV compared to the corresponding ventricle of the WT mice (Figure 4B) (B) RNAseq data show p38αβ cdKO

does not elevate ATF expression in the RV but only in the LV at P3. When these p38αβ cdKO mice enter P3, our RNAseq data indicate that ATF6 expression only varies in the LV but not the RV, which is inconsistent with our observed RV-specific proliferation and XBP1 variation. *p value* (WT vs. cdKO), * indicates $p<0.05$ and ** indicates $p<0.01$, n=3.

Figure 5

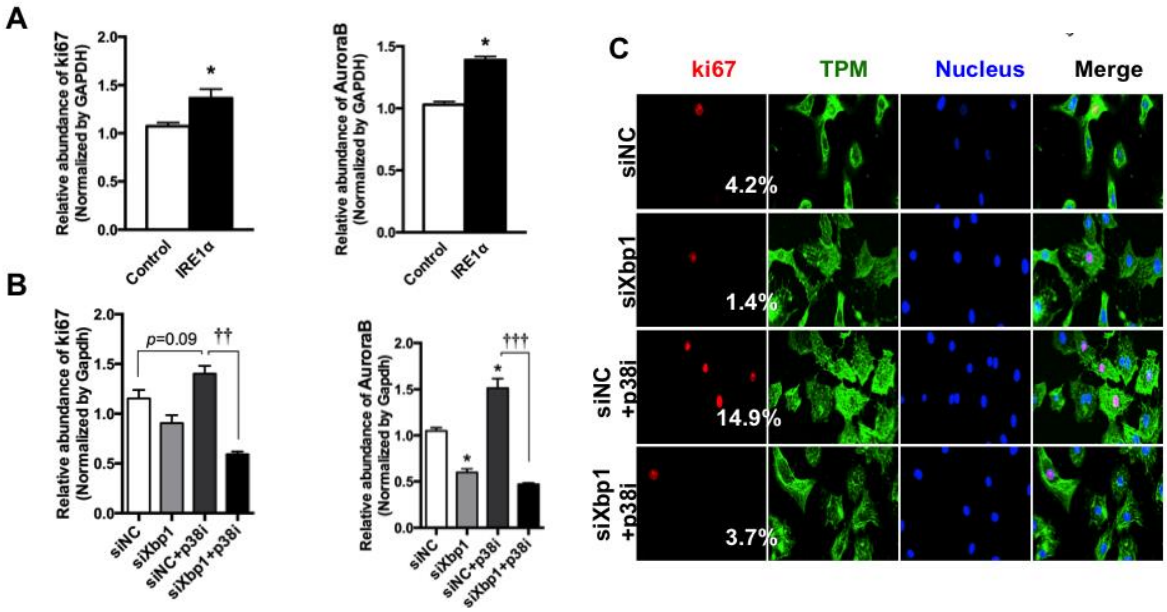

Figure 5. XBP1 knock down blunts the p38-inhibition-induced proliferation in NRVMs. (A) qPCR results show IRE1α overexpression promotes NRVM's mitotic activity. Ki67 and AuroraB were used as proliferation markers. (B) and (C) qPCR and immunostaining assays suggest that by infecting siRNA against XBP1 can blunt the p38-inhibition-induced proliferation in NRVMs. siXBP1 alone can suppress the basal mitotic activity of NRVMs, and can also attenuate the p38-inhibition-induced proliferation to the basal level. *p value* (WT

vs. cdKO), * indicates $p<0.05$, n=3. (siNC vs. siXBP1, siNC vs. siNC+p38i, siNC vs. siXBP1 + p38i), * indicates $p<0.05$, n>200. (siNC + p38i vs. siXBP1 + p38i), †† indicates $p<0.01$, and ††† indicates $p<0.001$.

Figure 6

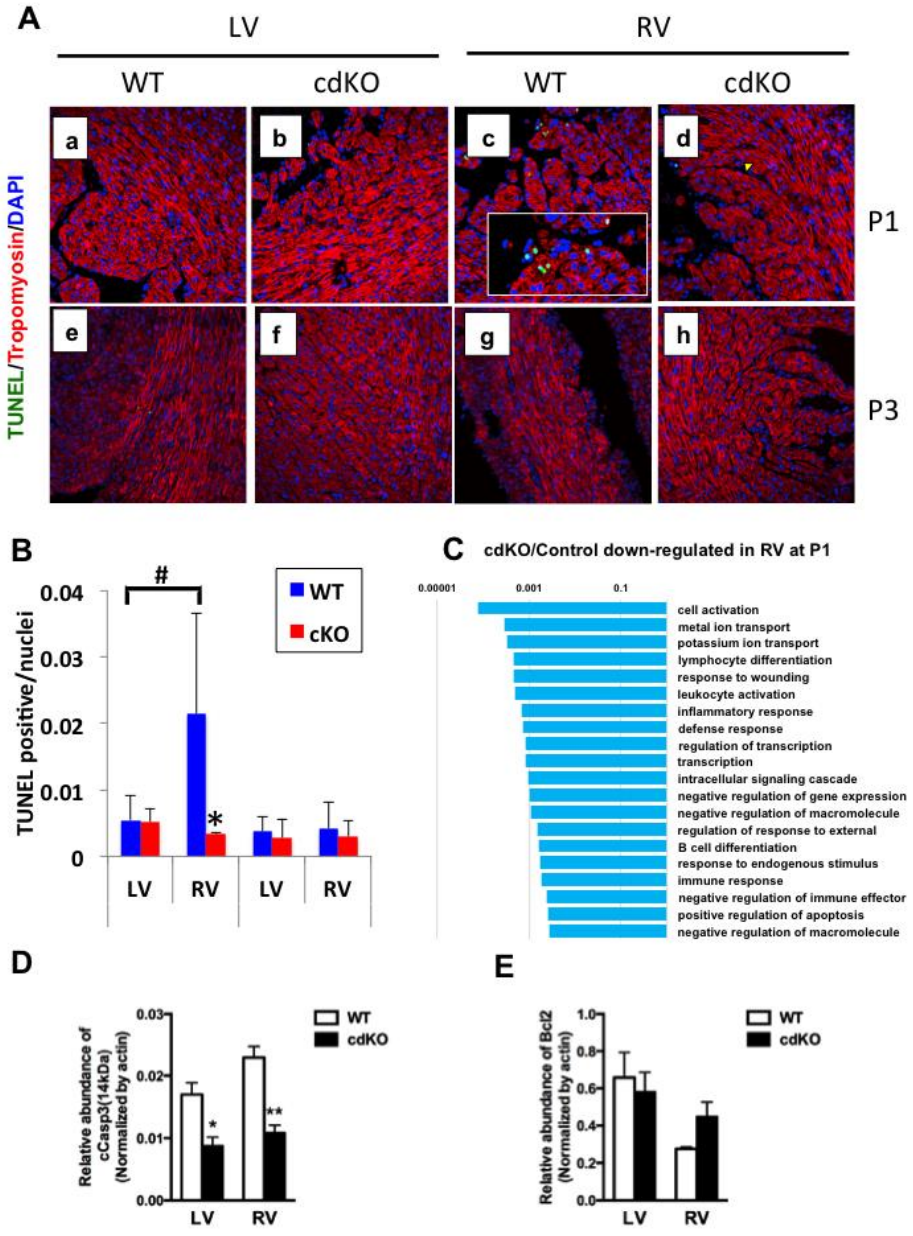

Figure 6. p38αβ cdKO suppresses the chamber-specific apoptosis in the RV at P1. (A) and (B) TUNEL assay and its quantification data suggest at P1, p38αβ cdKO can significantly suppress the originally high apoptotic activity in the RV but has no effect on the LV.

Terminal deoxynucleotidyl transferase dUTP Nick-End Labeling (TUNEL), tropomyocin and DAPI are used as biomarkers to detect the apoptotic cells (red), cardiomyocytes (green) and nuclei (blue) respectively. The ratio of TUNEL positive cardiomyocytes numbers to total cardiomyocytes numbers serves as an indicator to represent each ventricle's apoptotic activity. (C) RNA-seq data provide a list of genes undergoing down-regulation at P1 resulted from p38αβ cdKO. The list suggests that a set of genes exerting positive regulation of apoptosis in the RV were undergoing significant expression attenuation. But genes in similar pathways were not found to be down-regulated in the LV of the same mice at P1. (D) and (E) Western blot data suggest at P1, p38αβ cdKO significantly suppress the originally high apoptosis in the RV but not in the LV. cCasp3 and Bcl2 relative abundance (to actin) are used to represent the pro- and anti-apoptotic activities of cells respectively. In WT mice, the cCasp3 expression level in the RV is higher than that in the LV. In addition, knocking out p38αβ sequesters the expression of cCasp3 to more than two folds in both chambers, with that in the RV more significantly. Bcl2 has a just opposite expression trend as cCasp3: in the WT mice, Bcl2 abundance is over twice less in the RV than the LV; whereas after knocking out p38αβ, Bcl2 experiences a great expression rise in the RV, but this increase is not observed in the LV. *p value* (LV vs. RV) # indicates $p<0.05$; (WT vs. cdKO) * indicates $p<0.05$ and ** indicates $p<0.01$, n=3.

Figure 7

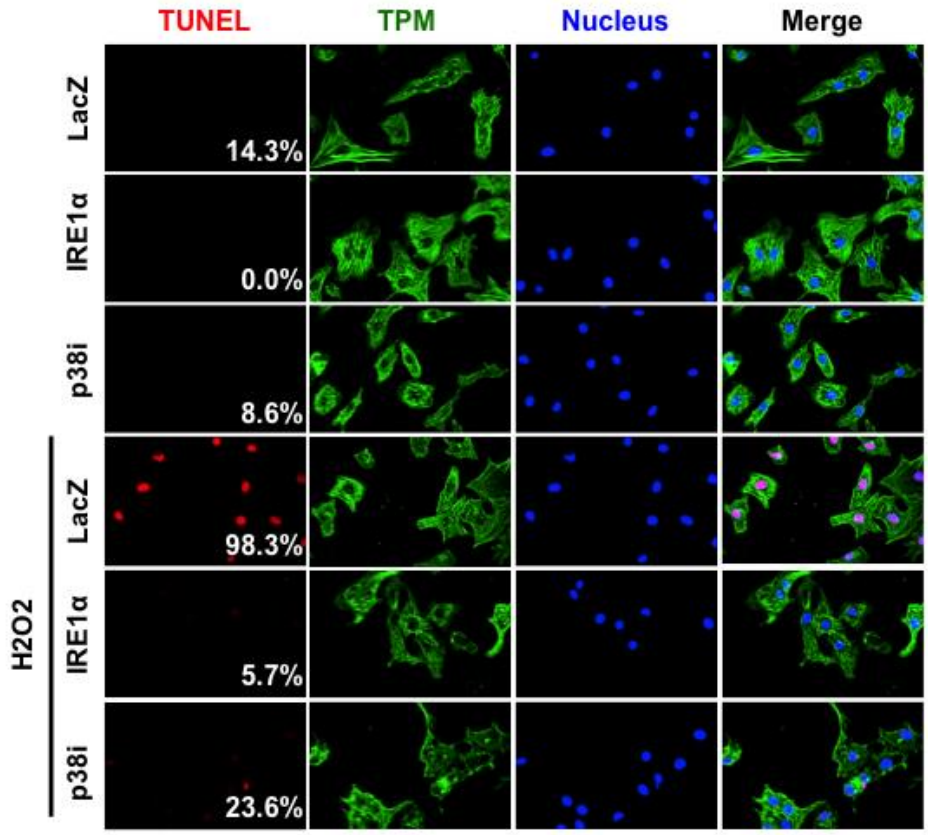

Figure 7. IRE1α overexpression attenuates NRVMs' apoptosis in both basal and stressful conditions, performing similarly to p38 inhibition does. TUNEL assay suggests that p38 inhibition can reduce NRVMs' basal apoptotic activity to almost a half extend compared to the non-treated (NT). p38 inhibition can reduce the percentage of apoptotic cells from 14.3% in the basal level to 8.6%; IRE1α overexpression can reduce this portion to 0%.

To simulate a stressful condition and induce cell apoptosis, a dose of 100 uM H2O2 was applied to NRVMs and cells were incubated for 0.5 hour before harvesting. Half-hour H2O2 treatment was able to generate an extremely high-level of apoptosis up to 98.3%. Strikingly, this death rate can be greatly reduced to as much as 23.6% once cells were applied with p38 inhibitor (applied one hour before H2O2 treatment); IRE1α overexpression can reduce this portion to 5.7%.

Figure 8

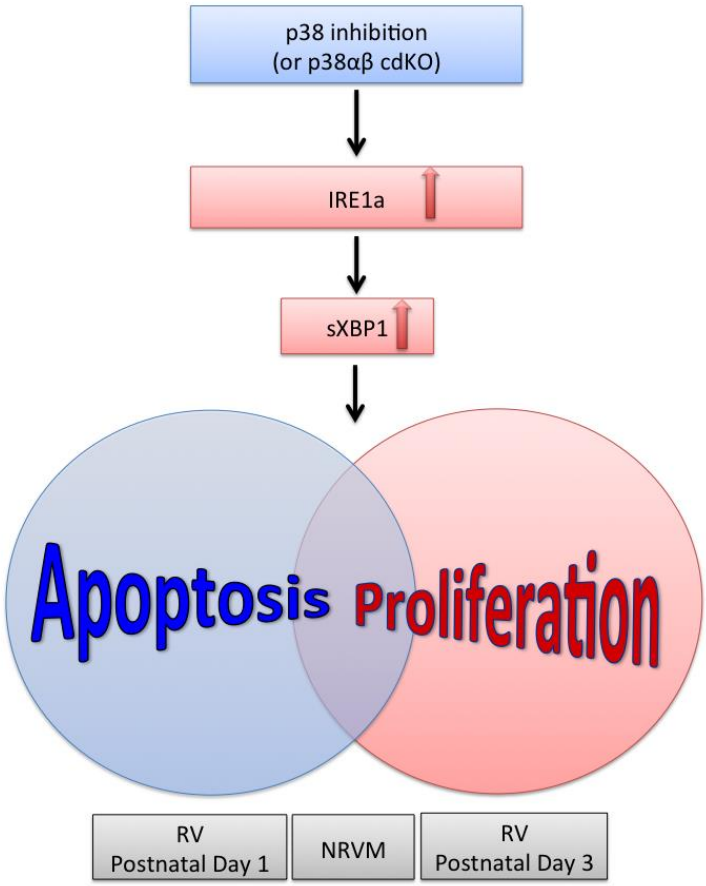

Figure 8. Model: p38 MAP kinase's dynamic and chamber-specific regulation of neonatal hearts remodeling via IRE1α. The proliferation and apoptosis pathways in this model share similar regulators of IRE1α and sXBP1, but then diverge into two branches to exert different modes of pro-survival effects. Specifically, after knocking out p38α and β isoforms in the RV, or once inhibiting p38 expression in the NRVMs, there is a universal induction in IRE1α expression and consequently an increasing XBP1 splicing level. However, this

enhanced XBP1 splicing will turn on different mechanisms to promote neonatal cardiomyocytes survival in the RV at different time point: this increased sXBP1 leads to an increment of proliferation only at P3, while results in reduced apoptosis only at P1. But both of these increased mitosis and suppressed apoptosis regulations exist in the NRVMs.

6. REFERENCES

Buttke, T. M., & Sandstrom, P. A. (1994). Oxidative stress as a mediator of apoptosis. *Immunology Today*. http://doi.org/10.1016/0167-5699(94)90018-3

Chen, Y., & Brandizzi, F. (2013). IRE1: ER stress sensor and cell fate executor. *Trends in Cell Biology*, *23*(11), 547–555. http://doi.org/10.1016/j.tcb.2013.06.005

Engel, F. B., Schebesta, M., Duong, M. T., Lu, G., Ren, S., Madwed, J. B., … Keating, M. T. (2005). p38 MAP kinase inhibition enables proliferation of adult mammalian cardiomyocytes. *Genes and Development*, *19*(10), 1175–1187. http://doi.org/10.1101/gad.1306705

Fan, T. J., Han, L. H., Cong, R. S., & Liang, J. (2005). Caspase family proteases and apoptosis. *Acta Biochimica et Biophysica Sinica*, *37*(11), 719–727. http://doi.org/10.1111/j.1745-7270.2005.00108.x

Fernandez, E., Siddiquee, Z., & Shohet, R. V. (2001). Apoptosis and proliferation in the neonatal murine heart. *Developmental Dynamics*, *221*(3), 302–310. http://doi.org/10.1002/dvdy.1139

Gamba, L., Harrison, M., & Lien, C.-L. (2014). Cardiac regeneration in model organisms. *Current Treatment Options in Cardiovascular Medicine*, *16*(3), 288. http://doi.org/10.1007/s11936-013-0288-8

Groenendyk, J., Sreenivasaiah, P. K., Kim, D. H., Agellon, L. B., & Michalak, M. (2010). Biology of endoplasmic reticulum stress in the heart. *Circulation Research*, *107*(10), 1185–

1197. http://doi.org/10.1161/CIRCRESAHA.110.227033

Han, D., Lerner, A. G., Walle, L. Vande, Upton, J., Xu, W., Hagen, A., … Ca, U. S. a. (2009). IRE1α Kinase Activation Modes Control Alternate Endoribonuclease Outputs to Determine Divergent Cell Fates. *Cell*, *138*(3), 562–575. http://doi.org/10.1016/j.cell.2009.07.017.IRE1

Hetz, C., & Glimcher, L. H. (2009). Fine-Tuning of the Unfolded Protein Response: Assembling the IRE1?? Interactome. *Molecular Cell*, *35*(5), 551–561. http://doi.org/10.1016/j.molcel.2009.08.021

Johnson, L. N., Noble, M. E. M., & Owen, D. J. (1996). Active and Inactive Protein Kinases : Structural Basis for Regulation, *85*(Table 1), 149–158.

Jopling, C., Suñè, G., Morera, C., & Belmonte, J. C. I. (2012). p38α MAPK regulates myocardial regeneration in zebrafish. *Cell Cycle*, *11*(6), 1195–1201. http://doi.org/10.4161/cc.11.6.19637

Lennon, S. V, Martin, S. J., & Cotter, T. G. (1991). Dose-Dependent Induction of Apoptosis in Human Tumor-Cell Lines by Widely Diverging Stimuli. *Cell Proliferation*, *24*(2), 203–214. http://doi.org/Doi 10.1111/J.1365-2184.1991.Tb01150.X

Liao, P., Georgakopoulos, D., Kovacs, a, Zheng, M., Lerner, D., Pu, H., … Wang, Y. (2001). The in vivo role of p38 MAP kinases in cardiac remodeling and restrictive cardiomyopathy. *Proceedings of the National Academy of Sciences of the United States of America*, *98*(21), 12283–12288. http://doi.org/10.1073/pnas.211086598

Lin, J. H., Li, H., Yasumura, D., Cohen, H. R., Zhang, C., Panning, B., … Walter, P. (2007). IRE1 signaling affects cell fate during the unfolded protein response. *Science (New York, N.Y.)*, *318*(5852), 944–9. http://doi.org/10.1126/science.1146361

Ma, X. L., Kumar, S., Gao, F., Louden, C. S., Lopez, B. L., Christopher, T. A., … Yue, T. L. (1999). Inhibition of p38 mitogen-activated protein kinase decreases cardiomyocyte apoptosis and improves cardiac function after myocardial ischemia and reperfusion. *Circulation*, *99*(13), 1685–91. http://doi.org/10.1161/01.CIR.99.13.1685

Monte, E., Mouillesseaux, K., Chen, H., Kimball, T., Ren, S., Wang, Y., … Franklin, S. (2013). Systems proteomics of cardiac chromatin identifies nucleolin as a regulator of growth and cellular plasticity in cardiomyocytes. *American Journal of Physiology. Heart and Circulatory Physiology*, *305*(11), H1624–38. http://doi.org/10.1152/ajpheart.00529.2013

Nebreda, a R., & Porras, a. (2000). p38 MAP kinases: beyond the stress response. *Trends in Biochemical Sciences*, *25*(6), 257–260. http://doi.org/10.1016/S0968-0004(00)01595-4

Pierre, N., Barb??, C., Gilson, H., Deldicque, L., Raymackers, J. M., & Francaux, M. (2014). Activation of ER stress by hydrogen peroxide in C2C12 myotubes. *Biochemical and Biophysical Research Communications*, *450*(1), 459–463. http://doi.org/10.1016/j.bbrc.2014.05.143

Porrello, E. R., Mahmoud, A. I., Simpson, E., Hill, J. A., Richardson, J. A., Olson, E. N., & Sadek,

H. A. (2011). Transient regenerative potential of the neonatal mouse heart. *Science (New York, N.Y.)*, *331*(6020), 1078–80. http://doi.org/10.1126/science.1200708

Porrello, E. R., & Olson, E. N. (2014). A neonatal blueprint for cardiac regeneration. *Stem Cell Research*. http://doi.org/10.1016/j.scr.2014.06.003

Romero-Ramirez, L., Cao, H., Nelson, D., Hammond, E., Lee, A., Yoshida, H., … Koong, A. C. (2004). Advances in Brief XBP1 Is Essential for Survival under Hypoxic Conditions and Is Required for Tumor Growth, (650), 5943–5947.

Rose, B. a, Force, T., & Wang, Y. (2010). Mitogen-activated protein kinase signaling in the heart: angels versus demons in a heart-breaking tale. *Physiological Reviews*, *90*(4), 1507–1546. http://doi.org/10.1152/physrev.00054.2009

Streicher, J. M., Ren, S., Herschman, H., & Wang, Y. (2010). MAPK-activated protein kinase-2 in cardiac hypertrophy and cyclooxygenase-2 regulation in heart. *Circulation Research*, *106*(8), 1434–1443. http://doi.org/10.1161/CIRCRESAHA.109.213199

Sun, H., Wang, N., Halkos, M., Kerendi, F., Kin, H., Guyton, R. A., & Zhao, J. V. Z. (2006). Postconditioning attenuates cardiomyocyte apoptosis via inhibition of JNK and p38 mitogen-activated protein kinase signaling pathways, 1583–1593. http://doi.org/10.1007/s10495-006-9037-8

Thorpe, J. A., & Schwarze, S. R. (2010). IRE1 α controls cyclin A1 expression and promotes cell proliferation through XBP-1, 497–508. http://doi.org/10.1007/s12192-009-0163-4

Thuerauf, D. J., Marcinko, M., Gude, N., Rubio, M., Sussman, M. a., & Glembotski, C. C. (2006). Activation of the unfolded protein response in infarcted mouse heart and hypoxic cultured cardiac myocytes. *Circulation Research*, *99*(3), 275–282. http://doi.org/10.1161/01.RES.0000233317.70421.03

Tsujimoto, Y. (1998). Role of Bcl-2 family proteins in apoptosis: Apoptosomes or mitochondria? *Genes to Cells*. http://doi.org/10.1046/j.1365-2443.1998.00223.x

Uygur, A., & Lee, R. T. (2016). Mechanisms of Cardiac Regeneration. *Developmental Cell*, *36*(4), 362–374. http://doi.org/10.1016/j.devcel.2016.01.018

Wang, Z. V, Deng, Y., Gao, N., Pedrozo, Z., Li, D. L., Morales, C. R., … Hill, J. A. (2014). Spliced X-Box Binding Protein 1 Couples the Unfolded Protein Response to Hexosamine Biosynthetic Pathway. *CELL*, *156*(6), 1179–1192. http://doi.org/10.1016/j.cell.2014.01.014

Wang, X. S., Diener, K., Manthey, C. L., Wang, S., Rosenzweig, B., Bray, J., … Yao, Z. (1997). Molecular cloning and characterization of a novel p38 mitogen-activated protein kinase. *The Journal of Biological Chemistry*, *272*(38), 23668–23674.

Wang, Y., Huang, S., Sah, V. P., Ross, J., Brown, J. H., Han, J., & Chien, K. R. (1998). Cardiac muscle cell hypertrophy and apoptosis induced by distinct members of the p38 mitogen-activated protein kinase family. *The Journal of Biological Chemistry*, *273*(4), 2161–2168. http://doi.org/10.1074/jbc.273.4.2161

Xu, T., Yang, L., Yan, C., Wang, X., Huang, P., Zhao, F., … Liu, Y. (2014). The IRE1α-XBP1

pathway regulates metabolic stress-induced compensatory proliferation of pancreatic β-cells. *Cell Research*, 1–4. http://doi.org/10.1038/cr.2014.55

Yokota, T., Ren, V., & Wang, Y. (2014). Chamber Specific Function of p38 MAP Kinases in Right Ventricle Development , Hypertrophy , and Dysfunction. *Circulation Research*, *115*, A287.

Yoshida, H., Matsui, T., Yamamoto, A., Okada, T., & Mori, K. (2001). XBP1 mRNA is induced by ATF6 and spliced by IRE1 in response to ER stress to produce a highly active transcription factor. *Cell*, *107*(7), 881–891. http://doi.org/10.1016/S0092-8674(01)00611-0

Zhou, M., Lu, G., Gao, C., Wang, Y., & Sun, H. (2012). Tissue-specific and nutrient regulation of the branched-chain α-keto acid dehydrogenase phosphatase, protein phosphatase 2Cm (PP2Cm). *Journal of Biological Chemistry*, *287*(28), 23397–23406. http://doi.org/10.1074/jbc.M112.351031